Electronic Supplementary Material (ESI) for Journal of Materials Chemistry A.

Electronic supplementary Information (ESI)

Exceptionally high-temperature in-air stability of transparent conductive oxide tantalum-doped tin dioxide

Matthias Krause,[a*] *Mareen Hoppe,*[a] *Carlos Romero-Muñiz,*[b] *Alvaro Mendez,*[a,c] *Frans Munnik,*[a] *Aurelio Garcia-Valenzuela,*[a] *Christian Schimpf,*[d] *David Rafaja,*[d] *Ramon Escobar-Galindo*[b]

[a] *Helmholtz-Zentrum Dresden – Rossendorf, Bautzner Landstraße 400, 01328 Dresden, Germany*

[b] *Departamento de Física Aplicada I, Escuela Politécnica Superior, Universidad de Sevilla, Virgen de África 7, 41011-Sevilla, Spain*

[c] *Nano4Energy SL, Madrid, Spain*

[d] *Institute of Materials Science, TU Bergakademie Freiberg, Gustav-Zeuner-Straße 5, 09599 Freiberg, Germany*

SI 1 (Supporting information): Analysis of the layer thickness of the series of 12 as-deposited SnO_2:Ta films and of the annealed samples #2 and #3 after thermal treatment in air

The thickness of the as-grown SnO_2:Ta thin films undergoes a systematic reduction of Δd = -1.5 ± 0.6 nm per deposition in a series of 12 samples (see Figure). The error of the thickness correlation function is σ_{n-1} = ± 4.2 nm.

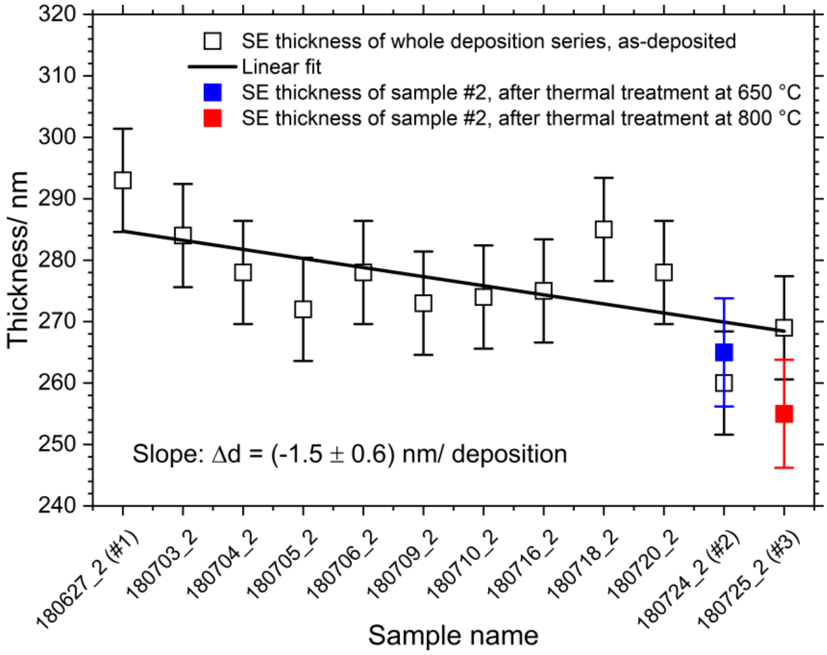

Thickness of the SnO_2:Ta thin films determined by spectroscopic ellipsometry (SE) prior to (☐) and after thermal annealing at 650 °C (🟦) and 800 °C (🟥), respectively. The linear fit is based on the thickness data after deposition.

As consequence, the lower thickness and areal density of sample #2 after thermal treatment is fully explained by the systematic and statistical deviations occurring within the deposition series. Thus, the thickness of sample #2 is unchanged during thermal in-air treatment at 650 °C. For sample #3, the thickness values before and after in-air annealing are still within the confidence range of ± 2σ_{n-1} = ± 8.4 nm (see table). From this finding, an annealing-independent thickness is concluded for this sample as well.

SnO_2:Ta sample	Ellipsometric thickness after deposition/ nm	Ellipsometric thickness after thermal treatment/ nm	Difference/ nm [%]
#1	293.0 ± 4.2	n.a.	n.a.
#2	260.0 ± 4.2	264.0 ± 4.2	+4 [+2]
#3	269.0 ± 4.2	255.0 ± 4.2	-14 [-5]
Calculated thickness decrease within the series of 12 samples/ nm	- 16.5 ± 4.2		

SI 2: Further details of the DFT calculations, views along the three crystallographic axes of the crystal structure of SnO_2:Ta (1 at.% Ta) and formation energies of the computed point defects

The equilibrium geometry of the all the different systems considered in this work were obtained after a full structural optimization following a conjugate gradient algorithm (see figure). All the atoms contained in the unit cells were free to relax in order to find their equilibrium positions. No restrictions in the lattice vectors were imposed during the minimization process. That is, changes in the shape and the volume of the unit cells were allowed. However, the minimal distortions found in the unit cells once the equilibrium geometries were achieved suggest that the original crystal symmetry remained after the incorporation of the point defects, as expected.

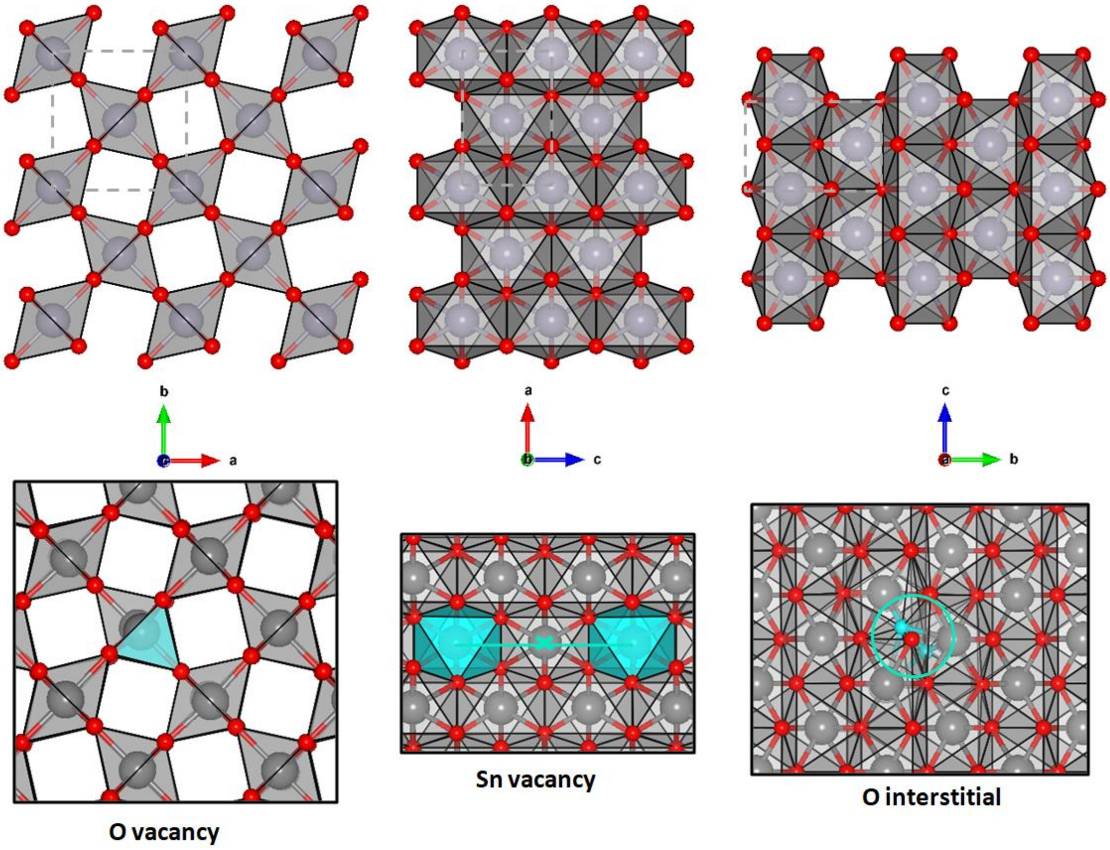

O vacancy

Sn vacancy

O interstitial

Views along the three crystallographic axes of crystal structure of rutile SnO2 (upper panel). The primitive unit cell is shown with a dashed gray line. In the lower panel we show the equilibrium geometries of the point defects studied in this work. Notice that some features of the defects are highlighted in cyan color to enhance their visualization.

About the structural details of the O_i and V_{Sn} point defects in SnO_2 and Ta-doped SnO_2, the following statements can be made. The rutile-type crystal structure of SnO_2 can be viewed as an arrangement of SnO_6 octahedra with Sn-O bond lengths of 2.06-2.08 Å. Oxygen vacancies do not produce any remarkable variation in the crystal structure while interstitial oxygen atoms and tin vacancies are able to produce noticeable changes. Interstitial oxygen atoms modify the coordination sphere of a single SnO_6 octahedron. The interstitial oxygen atom forms an oxygen dimer with a preexisting oxygen atom with larger Sn-O bond lengths of 2.21 Å, while the O-O distance of the dimer is 1.51 Å.

On the other hand, other Sn-O bond lengths of the new the 7-fold SnO_7 polyhedron are changed with respect the original SnO_6 configuration, ranging from 2.03 to 2.12 Å, i.e., the regular octahedron is slightly distorted. Remarkable distortions are also found in the presence of tin vacancies. They occur in the neighboring octahedra that deform, shortening their Sn-O bond lengths nearest to tin vacancy up to 2.02 Å while farther bond lengths enlarge to 2.12 Å.

The substitution of tin by tantalum also has some effect in the crystal structure. Essentially, the TaO_6 octahedron is smaller than SnO_6 one, with Ta-O distances of 2.00-2.01 Å. The further impact of point defects in SnO_2:Ta is essentially the same described for the undoped case, except for the case of oxygen vacancies. In this case, an extra shortening of the Ta-O distances is observed in the presence of the vacancy, leading to Ta-O bond lengths as short as 1.88 Å can be observed.

The formation energies of the calculated point defects are given in the following table, in comparison with the available values from ref. [32].

		Formation energies (eV)	
	System	This work	Williamson et al.
1	Pristine SnO_2	-	-
2	SnO_2:Ta	1.09	1.78
3	SnO_2-V_O	3.19	3.68
4	SnO_2:Ta-V_O-1 (near Ta)	5.00	5.55
5	SnO_2:Ta-V_O-2 (far from Ta)	4.54	
6	SnO_2–O_i	3.17	-
7	SnO_2:Ta-O_i-1 (near Ta)	3.68	-
8	SnO_2:Ta-O_i-2 (far from Ta)	4.19	-
9	SnO_2-V_{Sn}	9.38	10.07
10	SnO_2:Ta-V_{Sn}-1 (near Ta)	7.27	-
11	SnO_2:Ta-V_{Sn}-2 (far from Ta)	8.71	-

SI 3: Enlarged RBS spectra sections of the O edge of SnO_2 and Ta edge of SnO_2:Ta thin films: a) #1, after deposition, b) #2, after in-air annealing at 650 °C, c) #3, after in-air annealing at 800 °C.

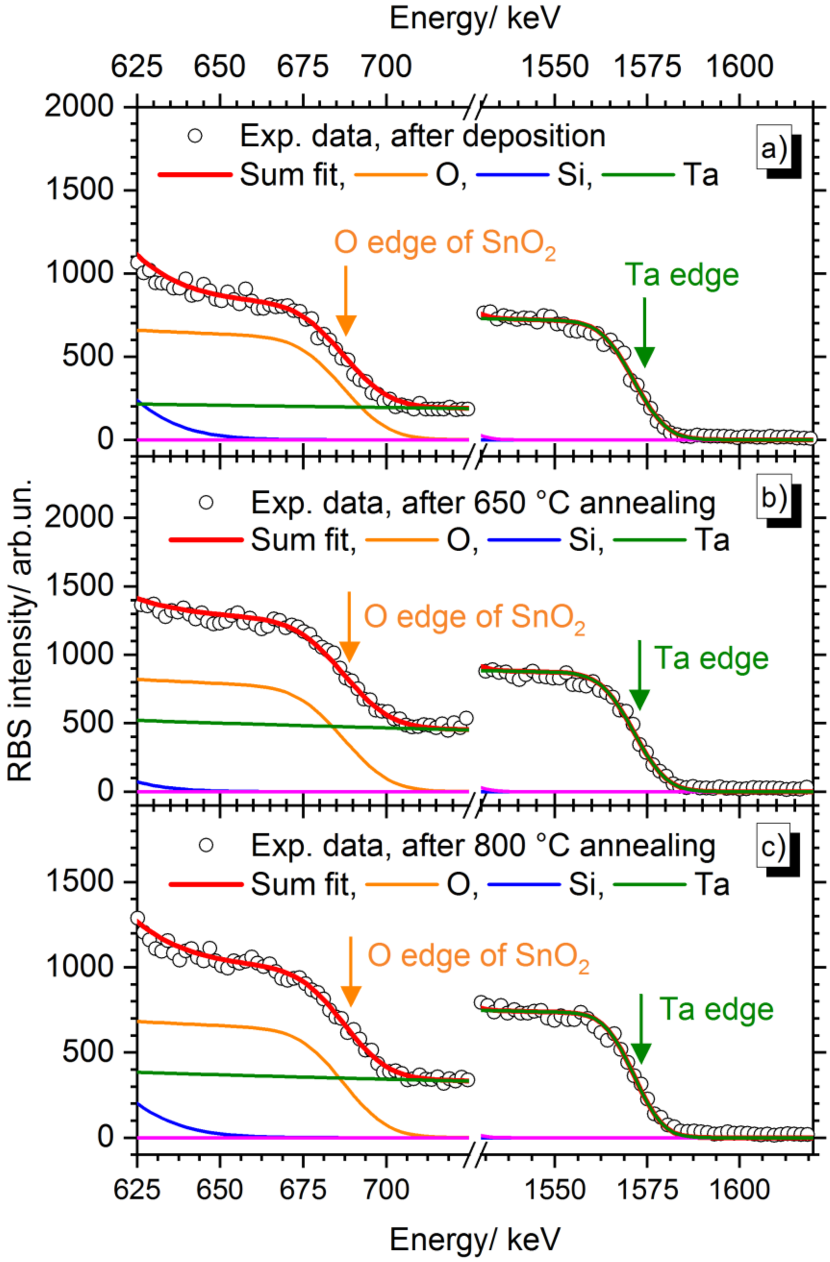

SI 4: Comparison of the transmittance and reflectance spectra of samples #2 (a, b) and #3 (c, d) after deposition and after in-air tempering at 650 °C and 800 °C, respectively.